Thermochimica Acta, 240 (1994) 67–77
Elsevier Science B.V., Amsterdam
SSDI 0040-6031(94)01720-2

The pyrolytic decomposition of aluminium-tri-*sec*-butoxide during chemical vapour deposition of thin alumina films

V.A.C. Haanappel, H.D. van Corbach, T. Fransen * and P.J. Gellings

University of Twente, Department of Chemical Technology, P.O. Box 217, 7500 AE Enschede, The Netherlands

(Received 14 June 1993; accepted 28 September 1993)

Abstract

The effect of the deposition temperature and the partial pressure of water on the thermal decomposition chemistry of aluminium-tri-*sec*-butoxide (ATSB) during metal organic chemical vapour deposition (MOCVD) is reported. The MOCVD experiments were performed in nitrogen at atmospheric pressure. The partial pressure of ATSB was 0.026 kPa (0.20 mmHg) and that of water was between 0 and 0.026 kPa (0–0.20 mmHg).

The pyrolytic decomposition chemistry of ATSB was studied by mass spectrometry at temperatures between 160 and 420°C. The effect of water on the homogeneous reaction products was studied at 270, 300, 330 and 370°C. The main products were 2-butanol, *n*-butane, 2-butanone, 1-butene and/or 2-butene, and water. The amount of by-products increased with increasing temperature. Water did not significantly affect the homogeneous product formation, whereas the heterogeneous deposition reaction was extensively reduced with increasing partial pressure of water, above 270°C.

From the type, amount and distribution of the products formed during the pyrolytic decomposition of ATSB, an attempt was made to establish the main decomposition mechanism: free radical, α-hydride elimination, or β-hydride elimination.

INTRODUCTION

Alumina films deposited by metal organic chemical vapour deposition (MOCVD) have increasingly found applications in a variety of technologies, including transistor fabrication, optical filters and coatings for corrosion protection [1]. During the metal organic chemical vapour deposition, the metal alkoxide (precursor) is transported into a reaction chamber where the chemical decomposition reactions result in the deposition of the desired product.

The MOCVD technique can be carried out at atmospheric or at reduced pressure. In general the deposition of thin films at reduced pressure gives better results because of the increase in the mass flux of gaseous reactants and products through the boundary layer to the substrate [1].

* Corresponding author.

0040-6031/94/$07.00 © 1994 – Elsevier Science B.V. All rights reserved

The deposition of alumina by MOCVD at atmospheric pressure has been studied by, among others, Ajayi et al. [2, 3] and Maruyama and Arai [4], preparing amorphous alumina films by using aluminium acetylacetonate (AAA). Other precursors, such as aluminium tri-isopropoxide (ATI) [5, 6], tri-methyl aluminium (TMA) [7] and aluminium hexa-fluoro-acetylacetonate (HFA) [8], have also been studied.

Alumina films deposited at reduced pressure were extensively investigated by Meinders [9], Sawada et al. [10], and Ishida et al. [11] using TMA. ATI as a precursor for low pressure MOCVD has been studied by Morssinkhof [12], Saraie et al. [13], and Yom et al. [14].

In this paper, the decomposition chemistry of aluminium-tri-*sec*-butoxide (ATSB) in nitrogen at atmospheric pressure is studied. The homogeneous reaction products were analysed by mass spectrometry. An attempt was made to establish the main decomposition mechanism from the products formed during the pyrolytic decomposition of ATSB.

EXPERIMENTAL DETAILS

Details of the equipment for the metal organic chemical vapour deposition (MOCVD) of thin alumina films have been described elsewhere [15]. The process conditions were: partial pressure of the ATSB, 0.026 kPa (0.20 mmHg); partial pressure of water, between 0 and 0.026 kPa (0–0.20 mmHg); furnace temperature, 160–420°C.

The residual gas analyses of the outlet gas stream were performed by a quadrupole mass spectrometer (SpectraMass-Dataquad), located at the exit of the reactor. The Dataquad provided monitoring of the current from the ion detector as a function of the mass–charge ratio (m/z). The mass spectrometer was connected to an Alcatel rotary pump, Model 2002B and a Balzers turbo molecular high-vacuum pump with electronic controller. Gas samples were drawn by the rotary pump into a stainless steel capillary. Samples were taken every minute until the gas composition reached a steady-state value. At each temperature and water concentration, the intensity of a number of characteristic peaks was measured.

The analysis of the mass spectra of several organic compounds requires a good knowledge of the chemical structure of the molecule as well as the chemical behaviour [16–18]. Every molecule detected by the mass spectrometer is represented by a series of peaks as a result of fragmentation. To avoid problems of overlap from gas compounds having the same mass value, mass values with no possible overlap were monitored [19]. The most important peaks for products of the pyrolytic decomposition of ATSB are listed in Table 1. It is clear that for 1- and 2-butene, the peak numbers and their relative intensities are practically identical. This means that in the following sections no distinction is made between these isomers.

TABLE 1

Main hydrocarbon peaks in the mass spectrum formed from possible reaction products with their cracking pattern from the thermal decomposition of ATSB [16–18]

Compound	Peak [a]					
	1st	2nd	3rd	4th	5th	6th
1-Butanol	31 (100)	41 (60)	43 (59)	29 (31)	42 (31)	–
2-Butanol	45 (100)	31 (19)	29 (15)	41 (10)	43 (10)	
2-Butanone	43 (100)	29 (25)	72 (17)	57 (6)	42 (5)	–
n-Butane	43 (100)	29 (44)	27 (37)	28 (33)	41 (28)	39 (13)
1-Butene	41 (100)	56 (39)	39 (35)	27 (31)	28 (29)	55 (18)
2-Butene	41 (100)	56 (45)	39 (45)	28 (22)	27 (22)	55 (16)

[a] Numbers in parentheses correspond to the approximate intensities relative to the base peak (1st ≡ 100). Underlined numbers correspond to the monitored peaks of the reaction products.

RESULTS

Decomposition of ATSB in nitrogen

Figure 1 shows a mass spectrum taken during the deposition of alumina. The peaks at $m/z = 1$ and 2 correspond to hydrogen (H^+, H_2^+), 14 and 28 to nitrogen (N^+, N_2^+), 16 and 32 to oxygen (O^+, O_2^+), and 17 and 18 to water (HO^+, H_2O^+). The peaks at $m/z = 45$, $m/z = 43$ and 72, $m/z = 43$, $m/z = 56$ and 39 were monitored continuously and correspond to 2-butanol, 2-butanone, n-butane, and 1- and 2-butene, respectively. These are the detectable by-products from the thermal decomposition reaction of ATSB.

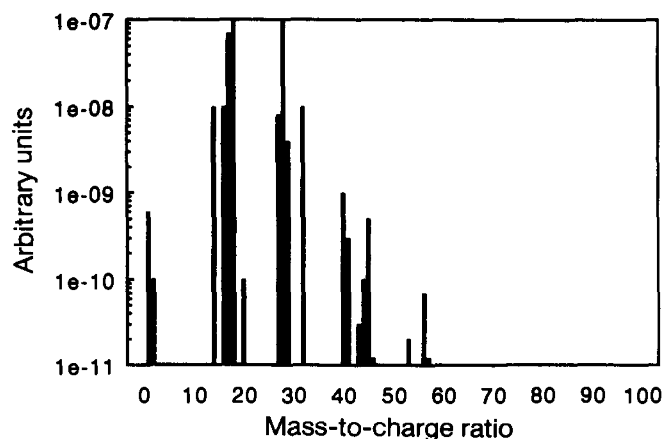

Fig. 1. An example of a mass spectrum of products from ATSB decomposition in a nitrogen atmosphere.

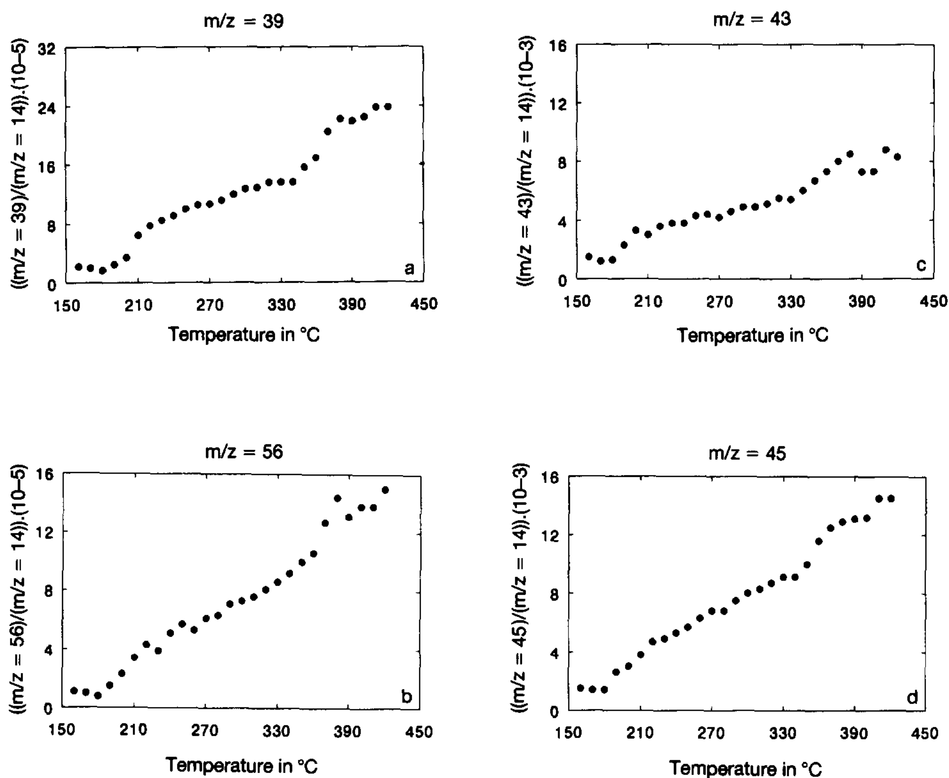

Fig. 2. Peak intensities (arbitrary units) as a function of the decomposition temperature of ATSB in N_2. a. $m/z = 39$, 1- and/or 2-butene. b. $m/z = 56$, 1- and/or 2-butene. c. $m/z = 43$, *n*-butane and 2-butanone. d. $m/z = 45$, 2-butanol.

Water was, of course, also found. Figures 2a and b show the relative peak intensities for the fragmentation patterns of 1- and/or 2-butene. The intensities of the peaks representing mass-to-charge ratios of 39 and 56 increase from 190°C. Because the ratio of the two peaks for 2-butanone at 43 and 72, also monitored by the mass spectrometer, is 100:17, the peak at $m/z = 43$ can be identified as a contribution from *n*-butane and 2-butanone. In Fig. 2c these relative peak intensities are given as a function of the temperature. Figure 2d shows the base peak intensity of 2-butanol with a mass-to-charge ratio of 45. All these figures show that the intensities increase with increasing decomposition temperature.

Decomposition of ATBS in nitrogen with small amounts of water

In addition to the thermal decomposition of ATSB, experiments were also carried out to study the effect of small amounts of water on the decomposition mechanism of ATSB at 270, 300, 330 and 370°C. The

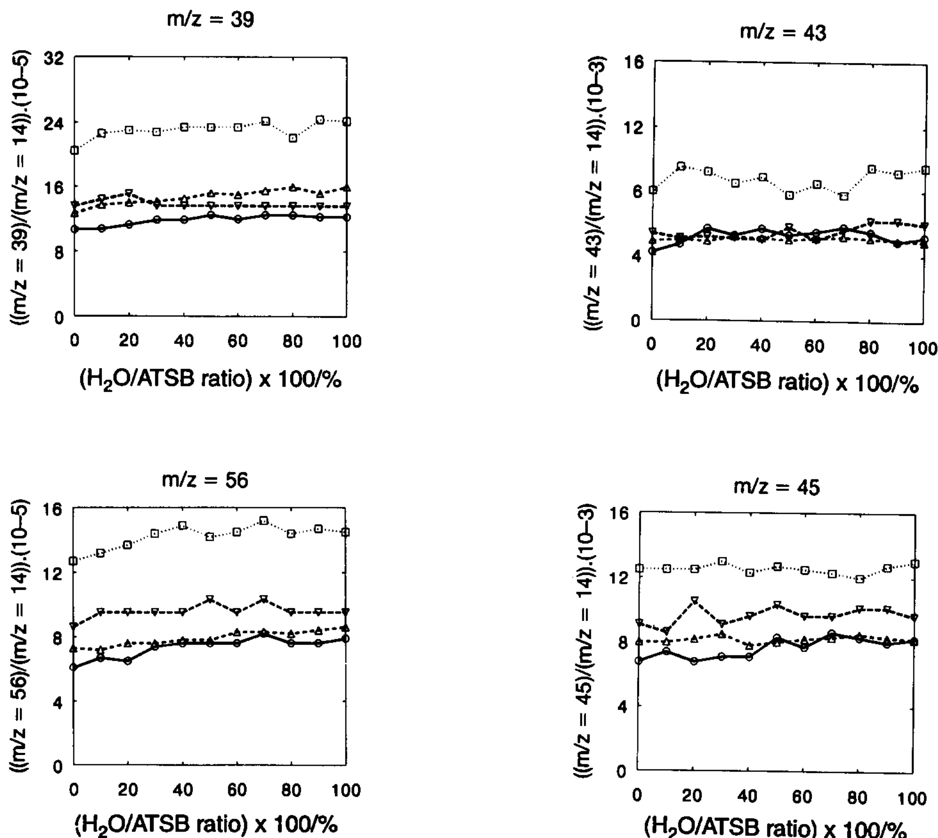

Fig. 3. Peak intensities (arbitrary units) as a function of the decomposition temperature of ATSB and water vapour pressure. a. $m/z = 39$, 1- and/or 2-butane. b. $m/z = 56$, 1- and/or 2-butene. c. $m/z = 43$, *n*-butane and 2-butanone. d. $m/z = 45$, 2-butanol. Symbols: ○, 270°C; △, 300°C; ▽, 330°C; □, 370°C.

amount of water ranged from 0 to 100% in ATSB, based upon the experiments described in ref. 21.

Figures 3a–d show the relative peak intensities of 1- and/or 2-butene ($m/z = 39$ and 56), 2-butanone with *n*-butane ($m/z = 43$) and 2-butanol ($m/z = 45$) as a function of the H_2O/ATSB ratio and furnace temperature. In general, a very small increase in the concentration of by-products was found with increasing water contents up to an H_2O/ATSB ratio of 100%.

DISCUSSION

As already mentioned, the main by-products from the pyrolytic decomposition of ATSB are 2-butanol, 2-butanone, 1-butene or 2-butene, and *n*-butane. Because the addition of small amounts of water did not change significantly the type and concentration of the products, the thermal decomposition mechanism in the gas phase is not altered by water. These results

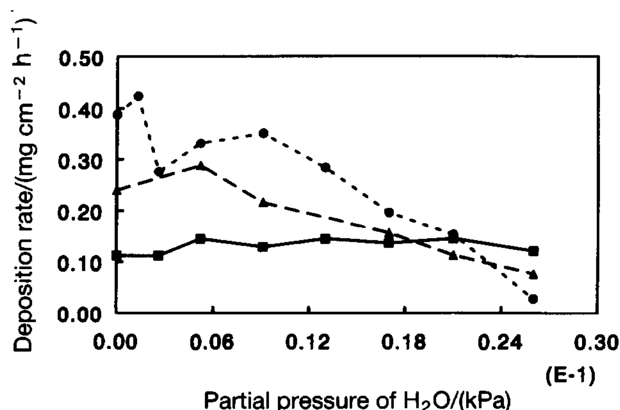

Fig. 4. Deposition rate of alumina as a function of the deposition temperature and water vapour pressure: ■, 280°C; ▲, 300°C; ●, 330°C.

are in contrast to those of Baryshnikov et al. [20] who found that water reacted effectively with the original alkoxide forming the corresponding alcohol. A probable explanation is the difference in residence time. Baryshnikov et al. [20] performed experiments under static conditions, which meant that the residence time of the alkoxide molecules in the reactor was large. For small residence times the reaction between water and alkoxide molecules may be negligible. However, small additions of water can affect the kinetics (heterogeneous reaction rate) to a much greater extent.

At low temperatures, no effect was observed if water was added up to an amount of 100% in ATSB. At higher temperatures ($\geq$300°C) the deposition rate decreases with increasing partial pressure of water. Figure 4 shows the deposition rate of alumina as a function of the water content and deposition temperature [21]. The number of interference rings, characteristic for the thickness uniformity of the deposited alumina films, increased significantly. Explanations for this might include a change in (1) the amount of adsorption sites (poisoning by water molecules); (2) atomic or molecular surface diffusion; (3) incorporation of water in the lattice; and (4) desorption of waste products.

From the literature [20–27], the thermal decomposition of alkoxides in the gas phase can be described by three different mechanisms: a free radical, a β-hydride elimination, and an α-hydride elimination mechanism.

The free radical mechanism has been discussed by, amongst others, Desu [22] and Barybin and Tomilin [23], investigating the decomposition chemistry of tetraethoxysilane (TEOS) and ATI, respectively. The free radical mechanism for ATI was based on the energy of displacement of electron pairs in the polar M–O bond [23, 24] and on the dissociation energy of the Al–O and O–C_3H_7 bonds [23]. Desu [22] used the bond energies within the TEOS molecule to explain the free radical mechanism. Figure 5 shows the

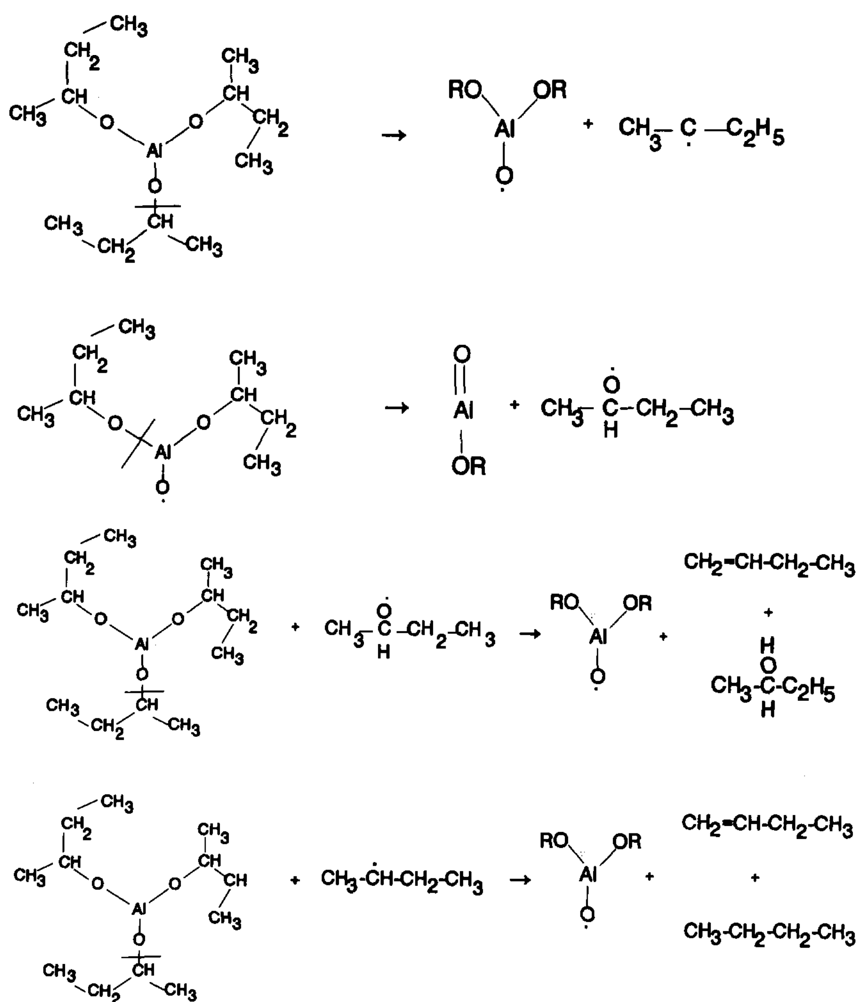

Fig. 5. Details of the free radical mechanism of the gas phase decomposition of ATSB (R is $CH_3-CH-CH_2-CH_3$).

details of the decomposition reaction of ATSB, assuming a free radical mechanism based on data from Desu [22] and Barybin and Tomilin [23]. It is suggested that the metal alkoxides form oligomers due to bridge formation of the alkoxide groups (between oxygen and the metal). This is explained by the tendency of the metal to expand its coordination number [25]. Barybin and Tomilin [23] also suggested that ATI forms dimers in the gas phase. In the first stage of the decomposition reaction, the oligomers form monomeric molecules by a rupture of the Al–O bridge bonds. Next, free radicals ($C_4H_9^{\cdot}$) are produced by a homolytic dissociation of the C–O bond. However, cleavage of the $Al-OC_4H_9$ bond leads to $C_4H_9O^{\cdot}$ radicals. Because the dissociation energy of the Al–O bond is much higher than that

of the O–C bond, it may be assumed that the first reaction takes place to a much greater extent. Korzo [26] reported that at high temperature not only the weak C–O bonds but also the Al–O bonds are broken. Therefore, in Fig. 5 two extreme dissociation paths are presented, showing not only the rupture of the C–O bond but also the cleavage of the Al–O bond. Consequently, the main radicals are $C_4H_9^{\bullet}$ and $C_4H_9O^{\bullet}$. As a result of the propagation (see Fig. 5) and termination reactions, these radicals react to yield the main by-products of the overall decomposition reaction: *n*-butane, 2-butanol, 3,4-dimethylhexane, 3,4-dimethyl-3-hexanol, and di-2-methyl-propyl-ether. Because only *n*-butane and 2-butanol were detected by mass spectrometry (the amount of the other compounds being below the detection level of the mass spectrometer), it may be assumed that the free radical mechanism does not play a dominant role in the overall decomposition mechanism of ATSB. Only when the larger organic compounds are formed to a much higher extent may the free radical mechanism partly explain the decomposition. Baryshnikov et al. [20], investigating the decomposition of ATI, did not find any product from a recombination reaction of free radicals either. This means that the free radical mechanism does not explain the decomposition of ATI. On the basis of these results it is concluded that the pyrolytic decomposition of ATSB occurs mainly by an α- or β-hydride elimination [20] and not by the free radical mechanism.

The second proposed decomposition mechanism (the β-hydride elimination) is based on data from Morssinkhof [12] and Baryshnikov et al. [20]. Figure 6 shows the details. Morssinkhof [12] described the β-hydride elimination by the occurrence of a rather stable monomeric six-membered ring with intramolecular bond formation between the Al–O group and the hydrogen attached to the β-carbon. Baryshnikov et al. [20] reported that in the vapour phase the molecules of ATSB were associated to dimers, which exist at temperatures up to 300–350°C. From the stable six-membered ring, the main products are 1-butene and/or 2-butene, and 2-butanol. Regarding the decomposition mechanism proposed by Baryshnikov et al. [20], the main products are 1-butene and 2-butanol. This β-hydride elimination mechanism becomes more important if the α-carbon atom becomes less accessible (steric hindrance) [27]. Because the alkyl groups in the ATSB molecules are rather large, it is suggested that α-hydride elimination is less important than β-hydride elimination. Of course, the α-hydride elimination mechanism may still play a role in the overall reaction.

The decomposition path of the α-hydride elimination, based on data from Desu [22], is presented in Fig. 7. The main products are *n*-butane, 1-butene, 2-butene, and 2-butanone. Baryshnikov et al. [20] found propene, propane, 2-propanol, water and acetone as the products of the thermal decomposition of ATI, indicative of a combined α- and β-hydride elimination mechanism. Morssinkhof [12] reported that only two compounds were detected in reasonable amounts by mass spectrometry: 2-propanol and propene. This

RO, Al, O, CH, C_2H_5, RO, H, CH_2 → O=Al-OR + H_2C=CH-CH_2-CH_3 + R-OH

RO, Al, O, CH, CH_3, RO, H, CH, CH_3 → O=Al-OR + H_2C-CH=CH-CH_3 + R-OH

Al, O, CH, C_2H_5, O, H, CH_2 → O=Al-O + H_2C=CH-CH_2-CH_3

H, OR, CH_3, CH, O, Et, Al, O, C-Et, CH_2, H, OR, Al, O, CH, Et, CH_2, OR, H → CH_2=CH-CH_2-CH_3 + R-OH

Fig. 6. Details of the β-hydride elimination mechanism of the gas phase decomposition of ATSB (R is CH_3–CH–CH_2–CH_3).

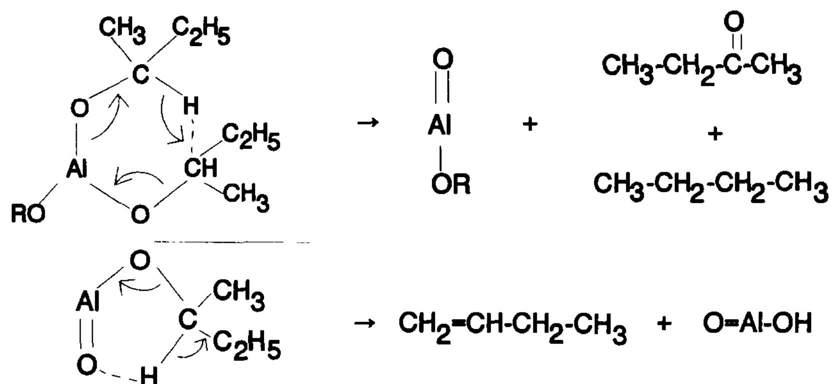

Fig. 7. Details of the α-hydride elimination mechanism of the gas phase decomposition of ATSB (R is CH_3–CH–CH_2–CH_3).

confirms the suggestion that the decomposition of ATI occurs mainly by a β-elimination mechanism. However, it is also known that the base peak of acetone ($m/z = 45(100)$) corresponds to the first minor peak of 2-propanol [16–18]. Nothing was reported by Morssinkhof [12] about the intensities of the minor peaks of acetone at $m/z = 58(23)$. Otherwise, two different gaseous compounds with similar mass-to-charge ratios may lead to a wrong interpretation. So, if acetone were present as one of the by-products, the α-hydride elimination mechanism might also play a role.

Based on the products formed during thermal cracking of metal organic compounds (alkoxides), the β-hydride elimination mechanism dominates the decomposition mechanism of ATSB. The other mechanisms, the free radical and the α-hydride elimination, may play only minor roles due to the large volume of the alkyl group of the metal organic compound ATSB.

CONCLUSIONS

MOCVD of alumina at atmospheric pressure in nitrogen from ATSB precursor yields 2-butanol, 2-butanone, n-butane, 1-butene (2-butene) and water as the main products. With increasing deposition temperature the amounts of all these compounds increase.

The addition of water reduces the heterogeneous reaction rate significantly at $T \geq 300°C$ and only at high water vapour pressures. The concentration ratios of the products formed in the gas phase does not change by the addition of water up to an H_2O/ATSB ratio of 1. A β-hydride elimination mechanism dominates the decomposition mechanism of ATSB. A free radical and an α-hydride elimination mechanism play only minor roles.

ACKNOWLEDGEMENTS

This research was supported by the Innovative Research Program on Technical Ceramics (IOP-TK) with financial aid from the Dutch Ministry of Economic Affairs.

REFERENCES

1 M. Ohring, The Materials Science of Thin Films, Academic Press, London, 1992.
2 O.B.A. Ajayi, M.S. Akanni, H.D. Burrow, J.N. Lambi, O. Osasona and B.P. Podor, Thin Solid Films, 138 (1986) 91.
3 O.B.A. Ajayi, M.S. Akanni, J.N. Lambi, C. Jeynes and J.F. Watts, Thin Solid Films, 185 (1990) 123.
4 T. Maruyama and S. Arai, Appl. Phys. Lett., 60(3) (1992) 322.
5 M.T. Duffy, J.E. Carnes and D. Richman, Metall. Trans., 2 (1971) 667.
6 C. Dhanavantri, R.N. Karekar and V.J. Rao, Thin Solid Films, 127 (1985) 85.
7 R.S. Ehle, B.J. Baliga and W. Katz, J. Electronic Mater., 12(3) (1983) 587.
8 D. Temple and A. Reisman, J. Electronic Mater., 19(9) (1990) 995.

9 L.G. Meinders, Thin Solid Films, 113 (1984) 85.
10 K. Sawada, M. Ishida, T. Nakamura and N. Ohtake, Appl. Phys. Lett., 52(10) (1988) 1672.
11 M. Ishida, I. Katakabe, T. Nakamura and N. Ohtake, Appl. Phys. Lett., 52(16) (1988) 1326.
12 R.W.J. Morssinkhof, The Deposition of Thin Alumina Films on Steels by MOCVD, Ph.D. Thesis, University of Twente, The Netherlands, 1991.
13 J. Saraie, J. Kwon and Y. Yodogawa, J. Electrochem. Soc., 132 (1985) 890.
14 S.S. Yom, W.N. Kang, Y.S. Yoon, J.I. Lee, D.J. Choi, K.Y. Seo, P.H. Hur and F.Y. Kim, Thin Solid Films, 213 (1992) 72.
15 V.A.C. Haanappel, H.D. van Corbach, T. Fransen and P.J. Gellings, Corrosion resistant coatings produced by metal organic vapour deposition using aluminium-tri-*sec*-butoxide, Thin Solid Films, 230 (1993) 138.
16 H. Budzikiewics, C. Djerassi and D.H. Williams, Interpretation of Mass Spectra of Organic Compounds, Holden-Day Inc., San Francisco, USA, 1964.
17 W. Benz, Mass Spektrometrie, Organischer Verbindungen (Methoden der Analyse in der Chemie), Akademische Verlagsgesellschaft, Frankfurt am Main, Germany, 1969.
18 F.W. McLafferty, Mass Spectrometry of Organic Ions, Academic Press, New York and London, 1963.
19 R. Iyer, D.L. Lile and C.M. McConica, J. Electrochem. Soc., 140(5) (1993) 1430.
20 Y.Y. Baryshnikov, I.L. Zakharov and G.I. Makin, Zh. Obshch. Khim., 60(6) (1990) 1350.
21 V.A.C. Haanappel, J.B. Rem, H.D. van Corbach, T. Fransen and P.J. Gellings, Properties of Alumina Films prepared by Atmospheric Pressure Metal-Organic Chemical Vapour Deposition using Small Amounts of Water, in preparation.
22 S.B. Desu, J. Am. Ceram. Soc., 72(9) (1989) 1615.
23 A.A. Barybin and V.I. Tomilin, Zh. Prikl. Khim., 49(8) (1976) 1699.
24 E.A. Shchupak, G.A. Domrachev and K.K. Fukin, Tr. Khim. Khim. Tekhnol., 3 (1968) 175.
25 D.C. Bradley, Chem. Rev., 89 (1989) 1317.
26 V.F. Korzo, Zh. Prikl. Khim., 49(1) (1975) 74.
27 R. Hofman, J.G.F. Westheim, V.A.C. Haanappel, T. Fransen and P.J. Gellings, Thermochim. Acta, 215 (1993) 329.